Analytical Modeling of Graphene Ribbons as Optical Circuit Elements

Amin Khavasi and Behzad Rejaei

***Abstract*— We demonstrate that graphene ribbons can be modeled as circuit elements, which have dual capacitive-inductive nature. In the subwavelength regime, the surface current density on a single graphene ribbon subject to an incident p-polarized plane wave is derived analytically and then it is extended to coplanar arrays of graphene ribbons by applying perturbation theory. It is demonstrated that even isolated graphene ribbons have capacitive properties and the interaction between them in an array only changes the capacitance. Finally, we propose an accurate circuit model for the ribbon array by applying appropriate boundary conditions.**

***Index Terms*— Graphene ribbon, circuit modeling, nanostructures.**

I. Introduction

GRAPHENE, a one-atom-thick sheet of carbon atoms arranged in a honeycomb lattice, has attracted a great deal of interest due to its exceptional electrical and optical properties, such as high thermal conductivity [1], gate-variable optical conductivity [2], controllable plasmonic properties [3] and high speed operation [4], among others. These properties make graphene a promising material for many applications, such as transformation optics [5], optical modulators [6], and transparent conducting electrodes [7].

Recently, periodic arrays of graphene ribbons and single graphene ribbon have been studied experimentally [8], [9] and numerically [10], [11]. It has been shown that periodic graphene patches possess dual inductive-capacitive nature [12], and thus the same property is for periodic graphene ribbons [13]. This bifunctional property could be useful in the implementation and design of tunable planar filters and metasurface conformal cloaks [14], [15].

The dual capacitive-inductive nature of graphene ribbons manifests itself in resonance features in transmission-reflection experiments through planar arrays of ribbons at THz frequencies [9]. At specific frequencies the reflection (and absorption) by the array increases significantly. However, to our knowledge, it is so far unclear whether these features are intrinsic to a single graphene ribbon or are caused by the interaction between ribbons in the array.

To address this problem, in this paper we shall first study the scattering of a p-polarized electromagnetic wave by a single graphene ribbon. We shall derive an analytical expression for the surface current density induced in a graphene ribbon in the subwavelength regime (i.e. the wavelength of the incident wave is much larger than the width of ribbon). The solution obtained possesses infinitely many intrinsic resonances which demonstrate that even a single graphene ribbon has both inductive and capacitive characteristics. Thus, unlike the multilayered stack studied in [12], the capacitive properties of the structure cannot be attributed to the interaction between graphene patches alone. We next turn to a periodic array of graphene ribbons and show that the resonance features of a single ribbon are still preserved apart from a shift caused by the electrostatic interaction between neighboring patches. This frequency shift will be calculated by means of perturbation theory. Moreover, the Rayleigh expansion, in combination with the surface current density on the graphene ribbons, will be used to determine the amplitude of the diffracted orders in the upper and lower homogenous media. Finally, we show that the array can be modeled with an effective admittance. The admittance is composed of infinite number of parallel R-L-C circuits, each representing a single mode of the graphene ribbon. Consequently, the proposed model correctly predicts multiple resonances of the structure.

The paper is organized as follows. In Sec. II, we derive an approximate analytical expression for the surface current density of a single graphene ribbon. In Sec. III, we extend our model to periodic arrays of graphene ribbons. In Sec. IV the calculation of diffracted orders and the circuit model of the structure are presented. We validate the proposed analytical model against full-wave numerical simulations [11]. Finally, conclusions are drawn in Sec. V. A time dependence of the form $e^{j\omega t}$ is assumed and suppressed throughout this study.

II. Current Distribution on a Narrow Graphene Ribbon

Consider a narrow graphene ribbon of width w (infinite along y) under normal incidence, as shown in Fig. 1. The surrounding medium is free space and the incident wave is p-polarized (magnetic field along y). The graphene ribbon is considered as a surface conductivity σ_s, computed within the random-phase approximation [16]:

$$\sigma_s = \frac{2e^2 k_B T}{\pi \hbar^2} \frac{j}{j\tau^{-1} - \omega} \log\left[2\cosh(E_F/2k_B T)\right] + \frac{e^2}{4\hbar}\left[H(\omega/2) - \frac{4i\omega}{\pi}\int_0^\infty \frac{H(\varepsilon) - H(\omega/2)}{\omega^2 - 4\varepsilon^2} d\varepsilon\right] \quad (1)$$

where e is the electron charge, E_F is the Fermi energy, $\hbar$ is the Plank constant, ω is the frequency, T = 300K is

Manuscript received December 16, 2013; revised February 17, 2014; accepted March 19, 2014. Date of publication April 11, 2014; date of current version April 16, 2014.

The authors are with the Department of Electrical Engineering, Sharif University of Technology, Tehran 11155-4363, Iran (e-mail: a.khavasi@yahoo.com; rejaei@sharif.ir).

Color versions of one or more of the figures in this paper are available online at http://ieeexplore.ieee.org.

Digital Object Identifier 10.1109/JQE.2014.2316133

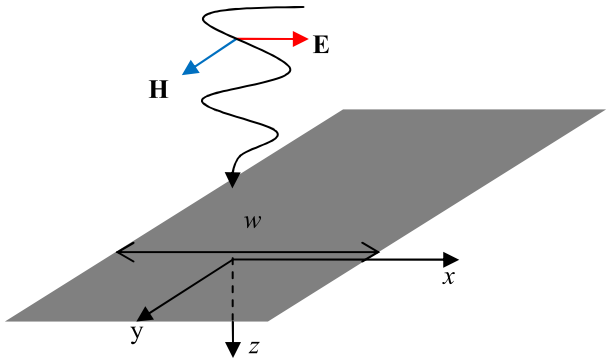

Fig. 1. A graphene ribbon of width w, illuminated by a normal incident p-polarized plane wave.

the temperature and τ is the relaxation time. The function $H(\varepsilon)$ is given by

$$H(\varepsilon) = \frac{\sinh(\hbar\varepsilon/k_B T)}{\cosh(E_F/k_B T) + \cosh(\hbar\varepsilon/k_B T)}$$

Due to the incidence of the p-polarized wave, a surface current density J_x will be induced on the ribbon in the x-direction. Once divided by σ_s, the surface current density must equal the total electric field on each point on the graphene surface. Therefore, one has [17]:

$$\frac{J_x(x)}{\sigma_s} = E_x^{ext}(x) - j\omega\mu_0 \int_{-w/2}^{w/2} G_0(x-x') J_x(x') dx' + \frac{1}{j\omega\varepsilon_0}\frac{d}{dx}\int_{-w/2}^{w/2} G_0(x-x')\frac{dJ_x(x')}{dx'}dx' \quad (2)$$

and

$$G_0(x-x') = \frac{1}{4j}H_0^{(2)}(k_0|x-x'|)$$

where $E_x^{ext}(x)$ is the x-component of the external electric field, and the last two terms on the right hand side of (2) represent the electric field generated in free space by the surface current J_x. Note that $H_0^{(2)}(x)$ is the zeroth order Hankel function of the second kind.

In the subwavelength regime where $k_0 w \ll 1$ one has

$$\frac{1}{4j}H_0^{(2)}(k_0|x-x'|) \approx -\frac{1}{2\pi}\ln(k_0|x-x'|) \quad (3)$$

Besides, due to the electrostatic nature of the problem, the third term on the right hand side will become much larger than the second, so the second term can be dropped:

$$\frac{J_x(x)}{\sigma_s} = E_x^{ext}(x) - \frac{1}{2\pi j\omega\varepsilon_0}\frac{d}{dx}\times\int_{-w/2}^{w/2}\ln(k_0|x-x'|)\frac{dJ_x(x')}{dx'}dx' \quad (4)$$

The above equation is of pure electrostatic nature as the 2nd term on its right hand side is simply the electrostatic field generated by a surface charge density $\rho_s = (-j\omega)^{-1} dJ_x/dx$.

TABLE I
THE FIRST THREE EIGENVALUE AND THEIR CORRESPONDING EIGENFUNCTIONS

Eigenvalue	Eigenfunction
$0.737\frac{\pi}{w}$	$\psi_1 = w^{-\frac{1}{2}}\left[1.2\sin(\cos^{-1}\frac{2x}{w}) - 0.106\sin(3\cos^{-1}\frac{2x}{w})\right]$
$1.753\frac{\pi}{w}$	$\psi_2 = w^{-\frac{1}{2}}\left[1.254\sin(2\cos^{-1}\frac{2x}{w}) - 0.302\sin(4\cos^{-1}\frac{2x}{w})\right]$
$2.748\frac{\pi}{w}$	$\psi_3 = w^{-\frac{1}{2}}\left[0.308\sin(\cos^{-1}\frac{2x}{w}) + 1.19\sin(3\cos^{-1}\frac{2x}{w}) - 0.484\sin(5\cos^{-1}\frac{2x}{w})\right]$

Furthermore, it may be rewritten as the Prandtl integro-differential equation [18]

$$-k_p(\omega)J_x(x) + \frac{1}{\pi}P\int_{-w/2}^{w/2}\frac{1}{x-x'}\frac{dJ_x(x')}{dx'}dx' = 2j\omega\varepsilon_0 E_x^{ext}(x) \quad (5)$$

Here $J_x(0) = J_x(w) = 0$[11], P denotes principal value integration, and

$$k_p(\omega) = -\frac{2j\omega\varepsilon_0}{\sigma_s}$$

is the (generally complex) wavenumber of the plasmonic wave propagating on an infinite sheet of graphene at the frequency ω [19].

To solve (5) consider the eigenvalue problem

$$\frac{1}{\pi}P\int_{-w/2}^{w/2}\frac{1}{x-x'}\frac{d\psi_n(x')}{dx'}dx' = k_n\psi_n(x) \quad (6)$$

where ψ_n is the n'th normalized eigenfunction ($\int_{-w/2}^{w/2}\psi_n^2(x)dx = 1$) and k_n is the corresponding eigenvalue. A method for calculating ψ_n and k_n by using Fourier expansion of eigenfunctions is presented in the Appendix. The first three eigenvalues and the corresponding (approximate) eigenfunctions are presented in Table 1. For higher order eigenvalues the following excellent approximation can be used:

$$k_n \cong (n-\frac{1}{4})\frac{\pi}{w},\ \psi_n = w^{-1/2}\sin(n\pi x/w)\quad n>3 \quad (7)$$

Returning to (5), we now expand the current density on the ribbon as follows:

$$J_x(x) = \sum_{n=1}^{\infty} A_n\psi_n(x) \quad (8)$$

which, after substitution in (5), leads to

$$A_n = \frac{2j\omega\varepsilon_0}{k_n - k_p(\omega)}\int_{-w/2}^{w/2} E_x^{ext}(x)\psi_n(x)dx \quad (9)$$

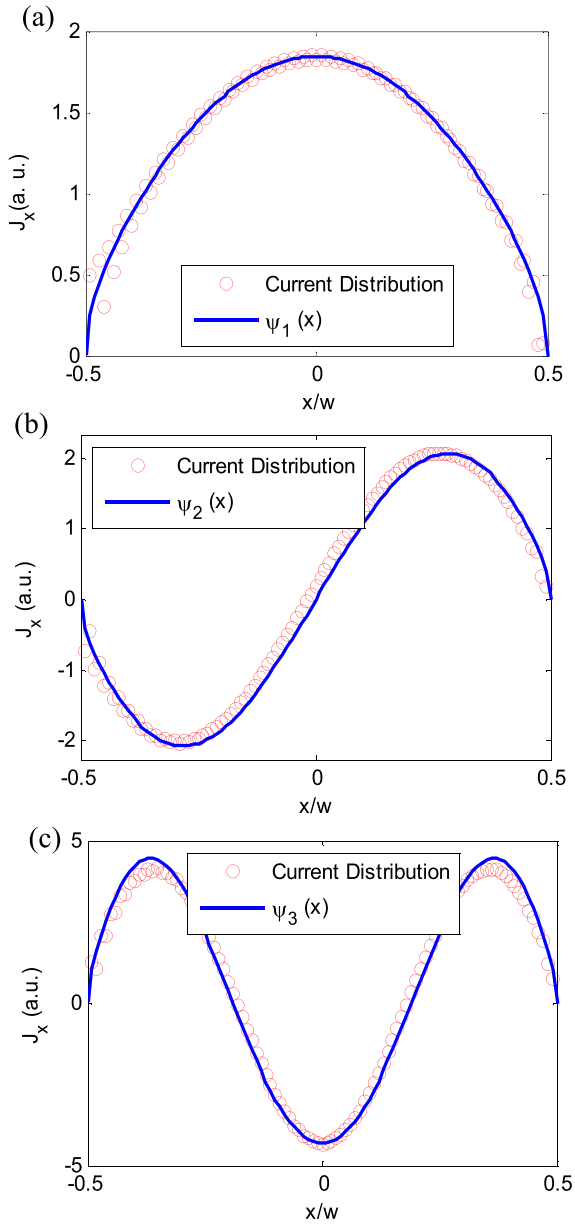

Fig. 2. Current distribution on the graphene ribbon for the (a) first, (b) second and (c) third mode, obtained by full wave simulation (circles). The corresponding approximate eigenfunctions from Table 1 are also plotted (solid line).

For normal plane wave incidence the external field is constant $E_x^{ext}(x) = E_x^{inc}$, so we have

$$A_n = \frac{2j\omega\varepsilon_0}{k_n - k_p(\omega)} S_n E_x^{inc} \tag{10}$$

where $S_n = \int_{-w/2}^{w/2} \psi_n(x)dx$. The latter quantity vanishes for even values of n as the corresponding ψ_n's are odd functions with respect to the center of the ribbon ($x = 0$).

Equation (8) shows that the current density on the ribbon exhibits infinitely many resonances at frequencies ω_n where $k_n = Rek_p(\omega_n)$. Near each resonance the distribution of current density will be given by the corresponding eigenfunction. These are, in fact, the quasi-static modes of the ribbon. Figure 2 (a), (b) and (c) show the current distribution of a graphene ribbon (circles) near its first three resonances obtained from full-wave electromagnetic simulations. For comparison the corresponding eigenfunctions from Table 1 (solid line) are also plotted on the same figures. Excellent agreement is observed between the numerical data and our quasi-static treatment. Note that the presence of resonances in the response of a graphene ribbon to an incident field demonstrates its dual inductive-capacitive character even in the absence of other graphene ribbons.

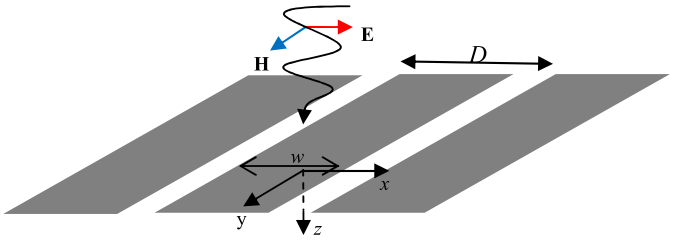

Fig. 3. Periodic array of graphene ribbons.

Finally, it should be mentioned that though the above equations were obtained for the case that the host medium is free space, they can be readily generalized to the case where the ribbon is sandwiched between two homogenous media with permittivities ε_1 and ε_2, respectively. Since the treatment is essentially electrostatic, it suffices to replace ε_0 with the effective permittivity [20] $\varepsilon_{eff} = (\varepsilon_1 + \varepsilon_2)/2$.

III. Extension to a Periodic Array of Ribbons

In this section, we extend the result obtained for a single ribbon to a periodic array of coplanar graphene ribbons of period D as shown in Fig. 3. We show that the interaction between the ribbons can be accurately taken into account by applying first order perturbation theory and modifying the eigenvalues in (6).

When the normally incident, p-polarized wave hits the array of parallel ribbons, surface currents flowing in the x-direction are once again induced on each ribbon. For each individual ribbon, equation (4) remains valid provided that the electric field induced by charges on neighboring ribbons is also included in its right hand side. Let the area of the i-th ribbon in the array be designated by $d_i < x < d_i + w$ and its current density by $J_{x,i}$. Then on the i-th ribbon (5) must be generalized as

$$-k_p J_{x,i}(x) + \frac{1}{\pi} P \int_{d_i}^{d_i+w} \frac{1}{x-x'} \frac{\partial J_{x,i}(x')}{\partial x'} dx' + \frac{1}{\pi} \sum_{l(\neq i)} \int_{d_l}^{d_l+w} \frac{1}{x-x'} \frac{\partial J_{x,l}(x')}{\partial x'} dx' = 2j\omega\varepsilon_0 E_x^{ext} \tag{11}$$

Since we are considering normal incidence, the external electric field E_x^{ext} is taken to be a constant and identical for all array elements. Besides, as the array is periodic and contains infinite number of ribbons, the distribution of current density on all array elements must be the same due to symmetry.

TABLE II
THE FIRST THREE EIGENVALUES OF (13) FOR DIFFERENT FILL-FACTORS, OBTAINED BY PERTURBATION THEORY

w/D	0.1	0.2	0.3	0.4	0.5	0.6	0.7	0.8	0.9
$q_1 w/\pi$	0.734	0.725	0.710	0.689	0.658	0.620	0.571	0.507	0.420
$q_2 w/\pi$	1.753	1.753	1.754	1.755	1.759	1.767	1.782	1.812	1.874
$q_3 w/\pi$	2.747	2.747	2.746	2.744	2.741	2.735	2.723	2.695	2.606

As a result (11) leads to the following equation for current distribution on an individual ribbon

$$-k_p J_x(x) + \frac{1}{\pi} P \int_{-w/2}^{w/2} \frac{1}{x-x'} \frac{\partial J_x(x')}{\partial x'} dx' + \frac{1}{\pi} \sum_{l(\neq 0)} \int_{-w/2}^{w/2} \frac{1}{x-x'+lD} \frac{\partial J_x(x')}{\partial x'} dx' = 2j\omega\varepsilon_0 E_{x,i}^{ext}(x) \quad (12)$$

valid in the interval $-w/2 < x < w/2$. It should be mentioned that the external field now also includes the radiated far fields of all the elements other than i.

Consider next the eigenvalue problem:

$$\frac{1}{\pi} P \int_{-w/2}^{w/2} \frac{1}{x-x'} \frac{\partial \phi_n(x')}{\partial x'} dx' + \frac{1}{\pi} \sum_{l=-\infty(\neq 0)}^{\infty} \int_{-w/2}^{w/2} \frac{1}{x-x'+lD} \frac{\partial \phi_n(x')}{\partial x'} dx' = q_n \phi_n(x) \quad (13)$$

Once the eigenfunctions ϕ_n and eigenvalues q_n are found, the solution will again be given by (8)-(10) except that ψ_n, k_n must be replaced by ϕ_n, q_n respectively. Instead of trying to directly solve (13), however, we treat the second term on its left hand side as an interaction-induced perturbation to the 'unperturbed' eigenvalue problem (6) for a single ribbon. It then follows from conventional perturbation theory that, up to the first order in the perturbation

$$q_n = k_n + \frac{1}{\pi} \sum_{l=-\infty(\neq 0)}^{\infty} \int_{-w/2}^{w/2} \psi_n(x) \int_{-w/2}^{w/2} \times \frac{1}{x-x'+lD} \frac{d\psi_n(x')}{dx'} dx dx' \quad (14)$$

which, after partial integration, may be written as

$$q_n = k_n - \frac{1}{\pi} \sum_{l=-\infty(\neq 0)}^{\infty} \int_{-w/2}^{w/2} \int_{-w/2}^{w/2} \times \ln\left|x-x'+lD\right| \frac{d\psi_n(x)}{dx} \frac{d\psi_n(x')}{dx'} dx dx' \quad (15)$$

where we have used $\psi_n(-w/2) = \psi_n(w/2) = 0$. Our calculations based on (15) show that higher order eigenvalues remain almost unchanged and, in practice, only the first three eigenvalues must be modified. The first three perturbed eigenvalues are given in Table 2 for different fill-factors (w/D). As for the eigenfunctions, we leave them unaltered and use $\phi_n \sim \psi_n$.

Consequently, for a periodic array of graphene ribbons, the surface current density of each graphene ribbon is obtained from (8) and (10) where k_n is replaced by the modified eigenvalues q_n calculated by (15). As in case of a single graphene ribbon, resonances will be observed but now near the modified frequencies found from $q_n = Re k_p(\omega_n)$. Take note that increasing the fill factor, which results in a smaller gap $(D - w)$ and stronger interaction between adjacent patches, mostly affects the lowest eigenvalue. The latter becomes smaller so that the corresponding resonance is shifted to lower frequencies (longer wavelengths).

IV. CIRCUIT MODEL

The existence of resonances for graphene ribbons in both isolated and array forms hints at its dual capacitive-inductive character from an electromagnetic point of view. It is therefore instructive to derive an equivalent circuit model which demonstrates these properties explicitly. Such a model will be derived below for an array of graphene ribbons by considering the scattering of a p-polarized plane wave.

The current distribution on each element in a periodic array of graphene ribbons was derived in the previous section. To analyze the scattering of the incident plane wave, however, we need to compute the electromagnetic fields generated by these currents in the surrounding homogenous media. The total field in these regions is given by the well-known Rayleigh expansion:

$$H_{1y} = e^{-j\beta_{10}z} + \sum_{n=-\infty}^{+\infty} r_n e^{j\beta_{1n}z} e^{-j\alpha_n x} \quad (16\text{-a})$$

$$E_{1x} = Y_{10}^{-1} e^{-j\beta_{10}z} - \sum_{n=-\infty}^{+\infty} Y_{1n}^{-1} r_n e^{j\beta_{1n}z} e^{-j\alpha_n x} \quad (16\text{-b})$$

for region I (z<0), and

$$H_{2y} = \sum_{n=-\infty}^{+\infty} \tau_n e^{-j\beta_{2n}z} e^{-j\alpha_n x} \quad (17\text{-a})$$

$$E_{2x} = \sum_{n=-\infty}^{+\infty} Y_{2n}^{-1} \tau_n e^{-j\beta_{2n}z} e^{-j\alpha_n x} \quad (17\text{-b})$$

for region II (z>0), where r_n and τ_n are the reflection and transmission coefficients, respectively, and

$$\alpha_n = \frac{2\pi}{D} n \quad (18\text{-a})$$

$$\beta_{in} = \sqrt{\frac{2\pi}{\lambda}\varepsilon_i - \alpha_n^2}, \quad i = 1, 2 \quad (18\text{-b})$$

$$Y_{in} = \frac{\omega\varepsilon_i}{\beta_{in}}, \quad i = 1, 2 \quad (18\text{-c})$$

In (18-b) λ is the free space wavelength. The z component of the wave vector, β_{in} is either negative real (propagating wave) or positive imaginary (evanescent wave).

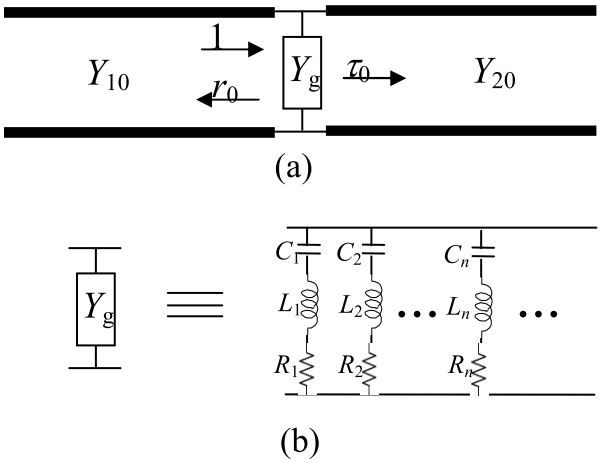

Fig. 4. (a) Proposed equivalent circuit for the structure shown in Fig. 3: the periodic array of graphene ribbons is modeled with a shunt admittance, Y_g, and the surrounding homogenous mediums are modeled with transmission lines. (b) The admittance representing the graphene ribbons can be regarded as infinite number of series R-L-C circuits that are parallel to each other.

Following boundary conditions should be applied in the boundary between the two regions where the graphene ribbons are deposited [21]:

$$E_{1x} = E_{2x} \tag{19-a}$$

$$H_{1y} - H_{2y} = J_x(x) \tag{19-b}$$

Substituting (16) and (17) in (19) we obtain, after some straightforward mathematical manipulations,

$$\sum_{n\neq 0}\left(1+\frac{Y_{2n}}{Y_{1n}}\right) r_n e^{-j\alpha_n x} + 1 - \frac{Y_{20}}{Y_{10}} + (1+\frac{Y_{20}}{Y_{10}})r_0 = J_x(x) \tag{20}$$

where J_x is given by (17) in which the external field is the incident field plus the radiated (reflected) field by the array. All reflection coefficients are easily calculated by multiplying both sides of (29) by $e^{-j\alpha_n x}$ and taking the integral over one period. For subwavelength regime, the zeroth reflection order is only propagating and its amplitude, r_0 is written as

$$r_0 = \frac{Y_g + Y_{20} - Y_{10}}{Y_g + Y_{20} + Y_{10}} \tag{21}$$

where according to (8), (9) and (21) Y_g reads as

$$Y_g = \sum_{n=1(\text{odd})}^{\infty}\left(\sigma_s^{-1} + \frac{q_n}{2j\omega\varepsilon_{eff}}\right)^{-1}\frac{S_n^2}{D} \tag{22}$$

In this relation even modes are absent as the corresponding values of S_n are zero (see section II).

The reflection coefficient given in (21), is the same as the reflection coefficient of the circuit shown in Fig. 4(a): two transmission lines with characteristic admittances Y_{10} and Y_{20}, and a shunt admittance Y_g, modeling regions I and II, and the array of graphene ribbons, respectively.

At sufficiently low frequencies and low temperatures where $\hbar\omega \gg 2E_F$ and $E_F >> 2k_BT$, 2nd term on the right hand side of (1) becomes negligible, and σ_s will be of the Drude form.

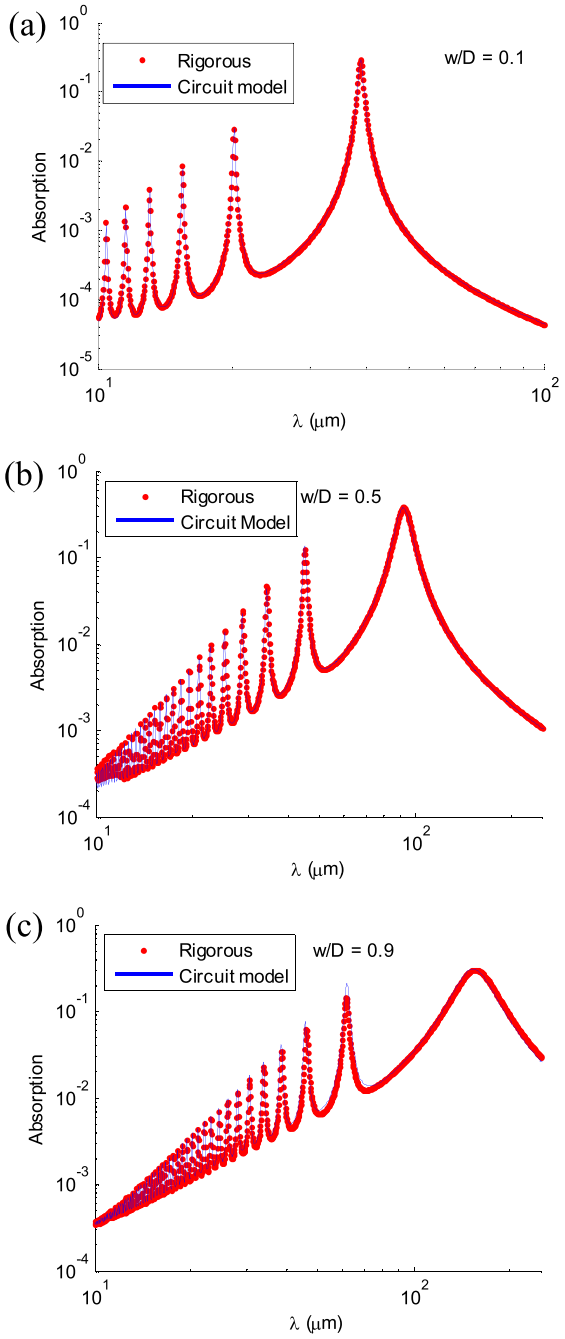

Fig. 5. Absorption spectra of periodic array of graphene ribbons with different values of ribbon width: (a) $w/D = 0.1$, (b) $w/D = 0.5$ and (c) $w/D = 0.9$. The results are obtained by using the proposed circuit model (solid curve) and full-wave simulations (dots).

Then each term in the above summation may be viewed as the admittance of a series R-L-C circuit with the resistance, inductance and capacitance of the n'th mode given by

$$R_n = \frac{D}{S_n^2}\frac{\pi\hbar^2}{e^2E_F\tau}, \quad L_n = \frac{D}{S_n^2}\frac{\pi\hbar^2}{e^2E_F}, \quad C_n = \frac{S_n^2}{D}\frac{2\varepsilon_{eff}}{q_n} \tag{23}$$

The total admittance of the ribbon array is thus the sum of the admittances of each mode as shown in Fig. 4(b). At high frequencies, where σ_s will not have the simple Drude form, the capacitance does not change while the resistance and

inductance are given by the frequency-dependent expressions

$$R_n = \frac{D}{S_n^2} Re\{\sigma_s^{-1}\}, \quad L_n = \frac{D}{S_n^2} \frac{Im\{\sigma_s^{-1}\}}{\omega} \tag{24}$$

Now, let us verify the accuracy of the proposed circuit model through a numerical example. Consider a periodic array of graphene ribbons whose period is $D = 8\mu$m deposited on a substrate with $\varepsilon_2 = 2.25\varepsilon_0$, and the incident medium is free space ($\varepsilon_1 = \varepsilon_0$). The charges relaxation time and Fermi energy are assumed to be: $\tau = 10^{-12}$ s, and $E_F = 0.2$ eV. The absorption of the structure is plotted as a function of the wavelength in Figs. 5(a), (b) and (c) for $w/D = 0.1$, 0.5 and 0.9, respectively. The dots show the rigorous results [11] and the solid curves are obtained by using the proposed circuit model. Excellent agreement is observed between the proposed model and the rigorous results.

It is obvious from these figures that the structure possess multiple resonances each corresponding to one of the series R-L-C circuits in the proposed model. These multiple resonances cannot be predicted with the previous work [12], modeling the structure with only one R-L-C admittance. Furthermore, as a result of the interaction between ribbons, which increases by increasing the fill-factor, the resonances are shifted to longer wavelengths. This effect is due to the reduction of the eigenvalues (q_n) of the odd modes as shown in Table 2. The widening of the resonances caused by increasing the fill-factor may also be understood in circuit terms. The width of a resonance is inversely proportional to the quality factor of its corresponding R-L-C branch which is given by $Q = (1/R_n)\sqrt{L_n/C_n}$. At long wavelengths where (23) is applicable, we have

$$Q = \frac{\tau e}{\hbar}\sqrt{\frac{q_n E_F}{2\pi\varepsilon_{eff}}} \tag{25}$$

Thus, a higher fill-factor will cause a smaller q_n and, in turn, a lower Q which manifests itself as a broader resonance.

V. Conclusions

We have derived an analytical expression for the surface current density of a graphene ribbon illuminated by a TM polarized plane wave. The expression has been derived under quasi-static approximation and it has been extended to periodic arrays of graphene ribbons by using perturbation theory. We demonstrated that interaction between the ribbons only changes the resonant frequency of the structure.

Moreover, we have proposed a circuit model for the structure consisting of parallel R-L-C circuits. This work confirms the dual capacitive-inductive properties of the graphene arrays, however, it suggests that even non-interacting ribbons have this dual feature. This is in contrast with the previous work [12] that attributed the capacitive property to the interaction of the ribbons. Also, multiple resonances and their quality factor are accurately predicted by the proposed model.

Our work gives a deeper insight to the physical properties of graphene ribbons and it may be useful for devising different novel devices such as perfect absorbers [22] and metasurface conformal cloaks [15].

Appendix: Solution of the Prandtl Eigenvalue Problem

In order to solve the eigenvalue problem (6) one may introduce the new variables

$$x = \frac{w}{2}\cos\theta, \quad x' = \frac{w}{2}\cos\theta' \tag{A.1}$$

which, after substitution in (6), lead to

$$\frac{2}{\pi w} P \int_0^{\pi} \frac{1}{\cos\theta' - \cos\theta} \frac{d\bar{\psi}_n(\theta')}{d\theta'} d\theta' = k_n \bar{\psi}_n(\theta) \tag{A.2}$$

with $\bar{\psi}_n(\theta) = \psi_n[(w/2)\cos\theta]$. We next expand $\bar{\psi}_n(\theta)$ in a Fourier sine series on the interval $0 < \theta < \pi$:

$$\bar{\psi}_n(\theta) = \sum_{p=1}^{\infty} A_p^n \sin(p\theta) \tag{A.3}$$

which, after substitution in (A.2) yields

$$\frac{2}{\pi w}\sum_{p=1}^{\infty} p A_p^n P \int_0^{\pi} \frac{\cos(p\theta')}{\cos\theta' - \cos\theta} d\theta' = k_n \sum_{p=1}^{\infty} A_p^n \sin(p\theta) \tag{A.4}$$

By using Glauert's identity [23]

$$P \int_0^{\pi} \frac{\cos(p\theta')}{\cos\theta' - \cos\theta} d\theta' = \frac{\pi \sin p\theta}{\sin\theta} \tag{A.5}$$

the above equation becomes:

$$\frac{2}{w}\sum_{p=1}^{\infty} p A_p^n \sin(p\theta) = k_n \sum_{p=1}^{\infty} A_p^n \sin\theta \sin(p\theta) \tag{A.6}$$

After multiplying both sides by $\sin(q\theta)$ and taking the integral from 0 to π, one obtains the generalized matrix eigenvalue problem

$$q A_q^n = \frac{k_n w}{\pi}\sum_{p=1}^{\infty} T_{qp} A_p^n \tag{A.7}$$

$$T_{qp} = \frac{1}{2}\frac{1-(-1)^{q+p-1}}{(q+p)^2-1} + \frac{1}{4}\frac{1-(-1)^{q-p+1}}{q-p+1}\left(1-\delta_{q-p,-1}\right) - \frac{1}{4}\frac{1-(-1)^{q-p-1}}{q-p-1}\left(1-\delta_{q-p,1}\right) \tag{A.8}$$

Solution of this problem with a finite number of coefficients gives the coefficients A_p^n and the eigenvalues k_n.

References

[1] Q. Bao and K. P. Loh, "Graphene photonics, plasmonics, and broadband optoelectronic devices," *ACS Nano*, vol. 6, no. 5, pp. 3677–3694, 2012.

[2] F. Wang *et al.*, "Gate-variable optical transitions in graphene," *Science*, vol. 320, no. 5873, pp. 206–209, 2008.

[3] F. H. Koppens, D. E. Chang, and F. J. G. de Abajo, "Graphene plasmonics: A platform for strong light-matter interactions," *Nano Lett.*, vol. 11, no. 8, pp. 3370–3377, 2011.

[4] F. Xia, T. Mueller, Y. Lin, A. Valdes-Garcia, and P. Avouris, "Ultrafast graphene photodetector," *Nature Nanotechnol.*, vol. 4, no. 12, pp. 839–843, 2009.

[5] A. Vakil and N. Engheta, "Transformation optics using graphene," *Science*, vol. 332, no. 6035, pp. 1291–1294, 2011.

[6] M. Liu *et al.*, "A graphene-based broadband optical modulator," *Nature*, vol. 474, no. 7349, pp. 64–67, 2011.
[7] S. Bae *et al.*, "Roll-to-roll production of 30-inch graphene films for transparent electrodes," *Nature Nanotechnol.*, vol. 5, no. 8, pp. 574–578, 2010.
[8] H. Yan *et al.*, "Damping pathways of mid-infrared plasmons in graphene nanostructures," *Nature Photon.*, vol. 7, no. 5, pp. 394–399, 2013.
[9] L. Ju *et al.*, "Graphene plasmonics for tunable terahertz metamaterials," *Nature Nanotechnol.*, vol. 6, no. 10, pp. 630–634, 2011.
[10] A. Y. Nikitin, F. Guinea, F. J. Garcia-Vidal, and L. Martin-Moreno, "Surface plasmon enhanced absorption and suppressed transmission in periodic arrays of graphene ribbons," *Phys. Rev. B*, vol. 85, no. 8, p. 081405, 2012.
[11] A. Khavasi, "Fast convergent Fourier modal method for the analysis of periodic arrays of graphene ribbons," *Opt. Lett.*, vol. 38, no. 16, pp. 3009–3012, 2013.
[12] Y. R. Padooru, A. B. Yakovlev, C. S. Kaipa, G. W. Hanson, F. Medina, and F. Mesa, "Dual capacitive-inductive nature of periodic graphene patches: Transmission characteristics at low-terahertz frequencies," *Phys. Rev. B*, vol. 87, no. 11, p. 115401, 2013.
[13] Y. Padooru, P. Chen, A. Yakovlev, and A. Alù, "Graphene metasurface makes the thinnest possible cloak in the terahertz spectrum," in *Proc. 7th Int. Congr. Adv. Electromagn. Mater. Microw. Opt.*, Sep. 2013.
[14] Y. R. Padooru, A. B. Yakovlev, P.-Y. Chen, and A. Alù, "Analytical modeling of conformal mantle cloaks for cylindrical objects using sub-wavelength printed and slotted arrays," *J. Appl. Phys.*, vol. 112, no. 3, p. 034907, 2012.
[15] Y. R. Padooru, A. B. Yakovlev, P.-Y. Chen, and A. Alù, "Line-source excitation of realistic conformal metasurface cloaks," *J. Appl. Phys.*, vol. 112, no. 10, pp. 104902-1–104902-11, 2012.
[16] A. Andryieuski and A. Lavrinenko, "Graphene metamaterials based tunable terahertz absorber: Effective surface conductivity approach," *Opt. Exp.*, vol. 21, no. 7, pp. 9144–9155, 2013.
[17] C.-T. Tai, *Dyadic Green Functions in Electromagnetic Theory*, vol. 272. New York, NY, USA: IEEE Press, 1994.
[18] N. I. Muskhelishvili, *Singular Integral Equations: Boundary Problems of Function Theory and Their Application to Mathematical Physics*. New York, NY, USA: Dover, 2008.
[19] M. Jablan, H. Buljan, and M. Soljačić, "Plasmonics in graphene at infrared frequencies," *Phys. Rev. B*, vol. 80, no. 24, p. 245435, 2009.
[20] O. Luukkonen *et al.*, "Simple and accurate analytical model of planar grids and high-impedance surfaces comprising metal strips or patches," *IEEE Trans. Antennas Propag.*, vol. 56, no. 6, pp. 1624–1632, Jun. 2008.
[21] D. J. Griffiths and R. College, *Introduction to Electrodynamics*, vol. 3. Englewood Cliffs, NJ, USA: Prentice-Hall, 1999.
[22] R. Alaee, M. Farhat, C. Rockstuhl, and F. Lederer, "A perfect absorber made of a graphene micro-ribbon metamaterial," *Opt. Exp.*, vol. 20, no. 27, pp. 28017–28024, 2012.
[23] H. Glauert, *The Elements of Aerofoil and Airscrew Theory*. Cambridge, U.K.: Cambridge Univ. Press, 1983.
[24] N. Marcuvitz, *Waveguide Handbook*. London, U.K.: IET, 1951.

Amin Khavasi was born in Zanjan, Iran, on January 22, 1984. He received the B.Sc., M.Sc., and Ph.D. degrees from Sharif University of Technology, Tehran, Iran, in 2006, 2008, and 2012, respectively, all in electrical engineering. Since then, he has been with the Department of Electrical Engineering, Sharif University of Technology, where he is currently an Assistant Professor.

His research interests include photovoltaics, plasmonics, and circuit modeling of photonic structures.

Behzad Rejaei received the M.Sc. degree in electrical engineering from the Delft University of Technology, Delft, the Netherlands, in 1990, and the PhD degree in theoretical condensed matter physics from the University of Leiden, Leiden, the Netherlands, in 1994. From 1995 to 1997, he served as a member of the Physics faculty at Delft University of Technology, where he carried out research on mesoscopic charge-density-wave systems. Between 1997 and 2010 he was with the Department of Electrical Engineering, Mathematics, and Computer Science at the Delft University of Technology. He is currently an Associate Professor at the Department of Electrical Engineering, Sharif University of Technology, Tehran, Iran. His research interests include electromagnetic modeling of integrated passive components, microwave magnetic devices, and magnetic metamaterials.